Plasma Waves Downstream of Weak Collisionless Shocks

F.V. Coroniti ,E.W. Greenstadt', S.L. Moses[1], E. J. Smith[2], B. T. Tsurutani[2]

[1]TRW S&EG, Redondo Beach, CA

[2]Jet Propulsion Laboratory, California Institute of Technology, Pasadena, CA

Abstract

In September 1983, the ISEE-3/ICE spacecraft made a long traversal of the distant dawnside flank region of the Earth's magnetosphere and had many encounters with the low Mach number bow shock, These weak shocks excite plasma wave electric field turbulence with amplitudes comparable to those detected in the much stronger bow shock near the nose region. Downstream of quasi-perpendicular (quasi-parallel) shocks, the E-field spectra exhibit a strong peak (plateau) at mid-frequencies (1-3 kHz); the plateau shape is produced by a low frequency (100-300 Hz) emission which is more intense behind quasi-parallel shocks. Polarization measurements made in the very steady magnetic field conditions downstream of two quasi-perpendicular shocks show that the low frequency signals are polarized parallel to the magnetic field, whereas the mid-frequency emissions are unpolarized or only weakly polarized, A new high frequency (10-30 kHz) emission which is above the maximum Doppler shift frequency is clearly identified as a separate wave component, High time resolution spectra often exhibit a distinct peak at high frequencies; this peak is often blurred by the large amplitude fluctuations of the mid-frequency waves, The high frequency component is strongly polarized along the magnetic field and vanes independently of the lower frequency waves.

1.0 Introduction

From September through December of 1983, the ISEE-3 spacecraft traversed the far dawn-side region of the magnetosheath and had multiple encounters with the bow shock [Greenstadt et al., 1990]. Since the shock normal is nearly orthogonal to the solar wind flow direction, the far flank shocks have low Alfven and magnetosonic Mach numbers. Thus, the ISEE-3 data set provides a unique opportunity to investigate the plasma, magnetic field, and plasma wave properties of collisionless shocks in a Mach number regime which has rarely been accessible to previous satellite studies. In this paper, we focus on plasma wave electric field measurements in the region immediately downstream of several typical quasi-parallel and quasi-perpendicular flank shocks. Strong shocks in the nose region of the magnetosheath [Rodriguez and Gurnett, 1975] and interplanetary shocks [Kennel et al., 1982] generate intense electric field turbulence in the

downstream region. The weak flank shocks might be expected to stimulate a significantly lower level of downstream wave noise. We find, however, that the electric field spectral amplitudes and spectral shapes detected behind the flank shocks are quite comparable to the wave properties observed behind the nose region shocks.

In the sub-solar region of the earth's bow shock, Rodriguez [1979] identified three types of electrostatic plasma waves which occurred in the magnetosheath: 1) a low frequency component with a peak near 100-300 Hz, well below the ion plasma frequency ($2\pi f_{pi} = (4\pi ne^2/m_i)^{1/2}$) and with a smoothly falling spectrum above the peak frequency; 2) an intermediate frequency component with frequencies between the ion and electron plasma frequencies ($f_{pi} < f < f_{pe}$) and a peak near 1 kHz; and 3) a high frequency component at the electron plasma frequency. The low frequency component resembles the wave spectra typically observed within the shock front [Rodriguez and Gurnett, 1975; Gurnett, 1985], whereas the intermediate and high frequency components had spectra which are similar to wave emissions in the upstream region. Rodriguez [1979] suggested that the intermediate frequency waves might be excited by narrow velocity spread electron beams as are believed to cause the similar upstream emissions. By comparing the voltages across antennas with different tip-to-tip lengths, Rodriguez [1979] concluded that the wavelengths of the magnetosheath turbulence exceeded 100 m across the entire frequency band from 40 Hz to 100 kHz. Since IMP 6 had a pair of orthogonal antennas and obtained the full waveform from O to 1,0 kHz, Rodriguez [1979] demonstrated that the electric field polarization in this frequency range was parallel to the magnetic field. At higher frequencies, Rodriguez and Gurnett [1975] used rapid sample (a measurement of a given frequency channel every 0.32 see) electric field amplitudes to show that the waves at 3.11 kHz were polarized along the field direction and stated that parallel polarization was a general property of the magnetosheath wave emissions.

Anderson et al. [1982] reported on two additional aspects of magnetosheath waves. Using the high time resolution capabilities of the ISEE 1 and 2 electric field spectrum analyser and wideband system, Anderson et al. [1982] discussed short duration emission spikes which spanned the frequency range from 100 Hz to 56 kHz. These spikes are a permanent feature of the nose

region magnetosheath and made the main contribution to the spectral density above 1.0 kHz. The HAM passive sounder measurements indicated that the e-folding time of the spikes was less than or comparable to the 8 msec time constant of the HAM receiver. The electric field spectrum analyzer showed that the spikes occurred simultaneously at all frequencies within the 50 msec resolution of the receiver. By comparing the electric field amplitudes as measured on antennas of different lengths, Anderson et al. [1982] concluded that the wavelengths of the spike emissions were less than 215 m. The most intense spikes have electric fields polarized in the plasma flow direction, whereas the lower amplitude spikes were polarized along the magnetic field.

The second magnetosheath emission discussed by Anderson et al. [1982] exhibits a characteristic falling and rising frequency structure which appears as a "U" or "festoon''-shape on an f-t diagram. These emissions occur below 2-3 kHz. At the higher frequencies, the electric field was polarized perpendicular to the magnetic field, whereas the lower frequencies were parallel polarized. From the amplitudes measured on the three ISEE antennas, Anderson et al. [1982] concluded that the wavelength was less than 73 m but greater than 30 m. The frequency-time structure of these emissions was explained by Gallagher [1985] as being produced by the response of a rotating antenna to polarized, Doppler-shifted waves with wavelengths less than the antenna length. For wavelengths longer than the antenna length, the amplitude response of the antenna is independent of the wavelength and depends only on the projection of the electric field along the antenna. For wavelengths less than the antenna length and for highly polarized signals, the antenna's amplitude response becomes a sensitive function of the rotation angle. Thus as the satellite spins, the antenna is sensitive to short wavelength signals only during certain intervals of rotation phase. By fitting the f-t shape of a festoon event, Gallagher [1985] deduced that for the observed (spacecraft frame) frequency range $0.65 < f \leq 2.5$ kHz, the emission wavelength varied in the range $5\ \lambda_D \leq \lambda \leq 56\ \lambda_D$; λ_D is the Debeye length based on the electron temperature ($\lambda_D = V_e/\omega_{pe}$ where $V_e = (T_e/M_e)^{1/2}$ and $\omega_{pe} = (4\pi ne^2/m_e)^{1/2}$) and was about 7 m during this event. From the linear relation between the observed frequency and wavenumber obtained by the detailed fitting of the festoon, Gallagher [1985] concluded that the emissions are Doppler shifted ion

acoustic waves. In a complimentary analysis of ISEE observations upstream of the shock, Fuselier and Gurnett [1984] used Gallagher's [1982] technique to deduce that the emissions between 0.5 and 10 kHz were ion acoustic waves with $k\lambda_D$ -1,

Recently Onsager et al. [1989] used the AMPTE swept-frequency receiver (SFR) measurements of magnetosheath electrostatic emissions to examine whether the entire frequency band between the ion and electron plasma frequencies could be explained as Doppler shifted ion acoustic waves. In the plasma rest frame, ion acoustic waves have a maximum frequency of f_{Pi} and usually have wave numbers restricted to $k\lambda_D < 1$ by Landau damping. In the spacecraft frame, the maximum Doppler shift occurs for waves propagating in the plasma flow direction, and the Doppler shift frequency is $f_D \cdot f_{pe} (V_{sw}/V_e) k\lambda_D$, where V_{sw} is the solar wind speed. Onsager et al. [1989] showed that the observed magnetosheath wave spectrum often extended to frequencies significantly above f_D but still below f_{pe}. They suggested that cold, parallel propagating, low density electron beams might excite electron beam modes with frequencies up to and even exceeding f_{pe}, thus explaining the bandwidth of the magnetosheath spectrum. They also noted that the electric field polarization should be predominantly parallel to the magnetic field, as observed by AMPTE.

In this paper we concentrate on both the high time resolution and the average spectral characteristics measured just downstream of two quasi-parallel and three quasi-perpendicular distant flank bow shocks. Section 2.0 presents the time averaged magnetic and electric field wave profiles for four flank shocks and discusses some high time resolution wave spectra that identify the presence of a new high frequency wave component. In Section 3.0 we present high time resolution magnetic field and wave spectral amplitudes for a quasi-perpendicular and quasi-parallel flank shock. In Section 4.0 we present the average downstream wave spectra for the flank shocks and compare these spectra with published electric field spectra measured behind the stronger nose shocks. Section 5.0 presents measurements of the wave electric field polarization. In Section 6.0 we summarize and briefly discuss our conclusions.

2.0 Electric Field Spectra - A High Frequency Component

The electric field wave spectra and magnetic field measurements were acquired by ISEE-3 on September 22 and 23, 1983, when the spacecraft was located about 83 R_E behind the earth and about 57 R_E on the dawnside flank. On these days ISEE-3 had many encounters with the bow shock in both the quasi-parallel and quasiperpendicular configurations, During these two days, the upstream solar wind speed was fairly steady at -400 km/see and the upstream density decreased slightly from 10 cm-3 on September 22 to 7 cm-3 on September 23. (The plasma measurements are from the LANL electron spectrometer.) We will discuss four shock crossings which are fairly typical of those encountered during this interval.

a. Quasi-parallel shock at 1706 UT on September 22, 1983

Figure 1 displays electric field wave measurements and the magnetic profiles for a pair of quasi-parallel shocks. The angle between the upstream magnetic field and the shock normal was $\theta_{Bn} = 19°$. The magnetosonic (fast) Mach number of the shocks is uncertain since ISEE-3 did not have the capability to make solar wind ion plasma measurements at this time. The upstream Alfven Mach number was 2.4 and the upstream electron $\beta = 8\pi nT_e/B^2 = 0.7$; the magnetic field (density) jump across the shocks was $B_2/B_1 = 1.4$ ($n_2/n_1 = 2.0$). The downstream region contains large amplitude magnetic fluctuations and fairly intense plasma wave emissions in the frequency range 316 Hz< f< 5.6 kHz; weak wave signals occur upto31.6 kHz. For a downstream flow speed of 400 km/sec and electron temperature of 1.8 x $10^{5°}$K, the maximum Doppler shift frequency is $f_D = 10\ k\lambda_D$ kHz.

The right-side of Figure 1 displays electric field amplitude spectra (volts/meter - $(Hz)^{1/2}$) over the range 17.8 Hz $\leq f \leq$ 100 kHz computed on several time scales; the top (bottom) curve represents the peak (average) spectral amplitude where appropriate. The top spectrum is a one-minute peak and average starting at 1704 UT downstream of the first shock. A broad, well-defined spectral peak occurs between 1.0- 2.0 kHz, which is close to the ion plasma frequency ($f^*; \approx 1$ kHz). Above the peak, the spectrum falls smoothly at higher frequencies with a slight change of slope at 10 kHz bending toward a flatter spectrum.

The four lower spectral curves in Figure 1 consist of two 3 second peak and average spectra measured between 1704:15-1704:18 (middle) and 1704:12-1704:15 (bottom). Just below each 3-second average, we show a spectrum made from a single measurement cycle of the plasma wave detector (a complete frequency spectrum is measured every 0.5 see); the single spectrum is one of the six such spectra that are averaged to produce the 3 second average spectrum. The 1704:15-183 second average spectrum is very similar to the 1 minute average spectrum at the top of Figure 1. The single measurement spectrum, however, is very different. The amplitudes below 56.2 Hz are about an order of magnitude lower than in the 3 second average spectrum so that the 1-3 kHz spectral peak is much clearer in the single spectrum. At 5.6 kHz the amplitude in the 3-second average spectrum is ten times higher than in the single spectrum. The single spectrum has a clear break in slope at 5.6 kHz and exhibits a gentle bump between 5.6 kHz and 56.2 kHz which indicates the presence of a separate high frequency emission. In the 3-second average spectrum this high frequency emission is masked by the gradual decrease of the amplitudes above the 1-3 kHz peak. For the spectra at the bottom of Figure 1, the amplitudes in the 3-second and single spectra at frequencies just below (316 Hz) and at the 1-1.78 kHz peak are nearly equal; and the spectral shapes at these frequencies are similar. Between 5.6 and 56.2 kHz, however, the single spectrum has a definite peak that is not apparent in the 3-second average spectrum, which only shows a subtle decrease in slope at these frequencies.

b. Quasi-parallel shock at 1551 UT, September 22.1982

Figure 2 displays electric field amplitudes from 178 Hz to 56.2 kHz, the magnetic field profile, and selected E-field spectra for a quasiparallel shock encountered about an hour earlier on September 22. The upstream magnetic field made an angle $\theta_{Bn} \approx 37$" with respect to a model shock normal, and the upstream Alfven Mach number of the shock was 2.3. The magnetic field (density) jump across the shock was $B_2/B_1 = 1.3$ ($n_2/n_1 = 1.8$), and the maximum Doppler shift frequency was $f_D \approx 9\ K\lambda_D$ kHz. The magnetic field structure and E-field amplitudes for this shock are very similar to those of the $\theta_{Bn} = 19^\circ$ shock in Figure 1.

On the right-hand side of Figure 2, the top curves are the 3-second peak and average E-field spectrum for the interval 15S 1:51-54 UT, which is about 30 seconds after the shock crossing. The average spectrum exhibits two reasonably well-defined peaks at 178 Hz and 1.0-1.78 kHz and falls smoothly at higher frequencies with a slight upward bending of the slope at 10 kHz. The next seven spectra are the single measurement cycles that were averaged to produce the top spectrum. The impulsive nature of the downstream waves is immediately apparent in that no two spectra are alike. A strong 178 Hz peak occurs in only three of the seven spectra. At 1 kHz, the largest and smallest amplitudes differ by an order of magnitude, and the shape of the spectrum near the 1.0-1.78 kHz peak is highly variable. At high frequencies, three of the spectra exhibit a distinct peak between 10.0 and 17.8 kHz, even though the 3-second average spectrum shows only a slight flattening in this frequency range. This high frequency peak can emerge both because the amplitudes near 3 -5.6 kHz diminish (as for the first spectrum) and because the 10.0 -17.8 kHz amplitudes increase. (The largest and smallest amplitudes at 17.8 kHz vary by a factor of five.)

The bottom 3-second average spectrum was obtained about one minute after the shock crossing and clearly exhibits a distinct high frequency peak of 10.0- 17.8 kHz. During this interval, the high frequency emission was sufficiently intense and steady to not be washed out in the average spectrum by the large fluctuations in the amplitudes of the waves at lower frequencies. These high frequency signals can be discerned in the E-field amplitude-time plots for each frequency channel (top left in Figure 2). The band from 10kHzto 31.6 kHz is enhanced at the shock and has a different appearance than the signals at lower frequencies, being somewhat less variable with smaller peak-to-average ratios.

c. Quasi-perpendicular shock at 0515 UT on September 23.19$3

In Figure 3 we present measurements for the θ_{Bn} = 62" quasi-perpendicular shock on September 23, 1983. The Alfven Mach number was 2.3, and the magnetic field (density) jump across the shock was B_2/B_1 = 1.7 (n_2/n_1 = 2). The lower solar wind density on September 23 reduced the downstream maximum Doppler shift frequency to f_D = 6.5 $k\lambda_D$ kHz. The magnetic profile of the quasi-perpendicular shock is much less variable than that of the previous two quasi-

parallel shocks. The E-field wave amplitudes exhibit a sharp onset at the shock and are significantly less variable than for the waves downstream of the quasi-parallel shock. The most intense waves again occur at mid-frequencies between 1.0 kHz and 3.16 kHz. At high frequencies between 10.0 kHz and 31.6 kHz, the wave amplitudes are very steady (low peak-to-average ratios) and have the appearance of being a separate component from the more variable wave emissions at lower frequencies.

The 3-second average E-field spectrum at the top of Figure 3 was calculated from the interval 05:14:08-11, about a minute before the shock encounter. The spectrum has a well-defined peak at 1.78 kHz and a small peak at 56 Hz. Just below, we display the six single sweep spectra that were averaged to produce the top spectrum. The 56 Hz peak is due to a strong burst which occurred in the fifth single spectrum. The spectral shape near the 1.78 kHz peak is highly variable, with only three of the six spectra exhibiting a sharp peak. Although again not apparent in the 3-second average spectrum, a high frequency peak or enhancement occurs in five of the six single spectra, At the bottom of Figure 3, we show an earlier 3-second average spectrum in which the high frequency emission appears as a distinct break in the slope rather as a clear peak.

d. Quasi-perpendicular shock at 0528 UT on September 23, 1983

The final example is a quasi-perpendicular θ_{Bn} = 76" shock that occurred at 0528 UT. The upstream solar wind parameters, the Alfven Mach number, magnetic field and density jumps, and maximum Doppler frequency were essentially the same as for the earlier0515 UT shock. At the shock, the mid-frequency wave amplitudes are strongly enhanced. The high frequency wave amplitudes also increase behind the shock and are temporally much steadier than either the downstream lower frequency waves or the high frequency upstream waves. Although the previous shocks discussed above had some very weak high frequency wave activity in their upstream regions, (the upstream region of the 1706 UT shock on September 22 may not have been sufficiently removed from the two shock ramps to be well sampled), the 0528 UT shock has a clearly associated, moderately intense upstream 10-31 kHz emission. The upstream electron plasma frequency was 24 kHz, so that the 10 kHz and probably also the 17.8 kHz signals are

below the plasma frequency. For the subsolar bow shock, the region downstream of the foreshock boundary often contains downshifted electron plasma oscillation [Etcheto and Faucheaux, 1984; Fuselier et al., 1985] which are highly impulsive emissions in the frequency range $0.1\ f_p \leq f \leq f_{pe}$. The high frequency waves upstream of the 0528 UT shock are probably in this category.

In the right-hand column of Figure 4, we show several 3-second average and single sweep spectra obtained in the downstream region, and at the bottom, a 3-second average spectrum from the upstream region. The first average spectrum exhibits a suggestion of peaks at mid-frequencies and high frequencies, and the single measurement spectrum just below it confirms the presence of a well-defined high-frequency peak. The second paired spectra also have two peaks. The third 3-second average spectrum has a large peak at 1.78 kHz, with a sufficiently intense high-frequency tail that the 10-31 kHz emission is not apparent. However, of the two single measurement spectra (shown below) which are included in calculating the average spectrum, the second spectrum clearly shows the high frequency peak. For comparison, the last spectrum is of the downshifted upstream plasma oscillations. The peak amplitudes of the upstream high frequency emissions are higher than the downstream amplitudes.

e. Conclusion

For the sub-solar bow shock, Onsager et al. [1989] demonstrated that the magnetosheath frequency spectrum extended to well-above the maximum Doppler shift frequency and suggested that these high frequency waves could be generated by parallel cold electron beams. The above analysis of magnetosheath spectra for the flank bow shock showed that a distinct high frequency wave emission extends from near the maximum Doppler shift frequency to below the electron plasma frequency. A similar spectral component is evident in Rodriguez's [1979] high time resolution spectra but was not noted in that paper. Thus, we conclude that the wave spectrum between the maximum Doppler shift and electron plasma frequencies is not necessarily produced by the same mechanism which generates the emissions at lower frequencies.

3.0 High Time Resolution E-Field Amplitudes

The single spectra displayed in the last section indicate that the E-field emissions in the magnetosheath are highly structured, In this section we examine the magnetosheath E-field amplitudes at the highest time resolution (0.5 second per spectrum) for two 90-second intervals downstream of a quasi-parallel and quasi-perpendicular shock. Despite the very different temporal behavior of the magnetic field behind these shocks, the E-field emissions are quite similar.

The top four panels of Figure 5 present the unaveraged, 1/6 second per vector magnetic field components and magnitude from 1703 UT to 1704:30 UT downstream of the 1706 UT quasi-parallel shock on September 22, 1983. Except for the substantial dip near 1703:15 UT, the field magnitude is fairly steady near 13 nT with fluctuations of ±2 nT. The BY component, essentially in the shock normal direction, exhibits somewhat more variability, but is still fairly steady. The x and z components, however, have fluctuations of ±10 -12 nT, i.e., of order the total field magnitude. Thus, even a very low Mach number, weak quasi-parallel shock generates order one large amplitude rotational turbulence in its downstream flow.

The lower panels in Figure 5 display the E-field spectral amplitudes in the frequency channels from 178 Hz to 5.6 kHz, At low and intermediate frequencies (1.0 to 5.6 kHz) the amplitudes can vary by one to two orders of magnitude between successive 0.5 second measurements. The decreasing portion following some of these rapid amplitude increases exhibits a temporal exponential decay which is characteristic of the instrument response to signals that persist for less than the 0.5 second measurement cycle. The instrumental decay is particularly evident in the 560 Hz channel which has a longer time constant than the other channels. Although some of the impulsive emissions are broadband with coincident peaks in all channels from 178 Hz to 5.6 kHz, both the low and intermediate frequency bands can independently have strong peaks. At higher frequencies, the amplitude fluctuations are significantly smaller, rarely being larger than a factor of 2-10, and are usually uncorrelated with variations in the lower frequency channels. The difference in temporal properties of the high frequency and low frequency emissions further

strengthens our earlier conclusion that the high frequency signals represent a separate spectral component.

Figure 6 presents high resolution magnetic field and E-field wave measurements for a quasi-perpendicular flank shock at 0622:41 UT encounter on September 23, 1983. The shock had an Alfven Mach number of MA = 2.46 and θ_{Bn} = 67". The shock ramp is quite sharp, even though the upstream region contained significant high frequency magnetic fluctuations. The downstream region is very quiet with only ±1 nT variations in all magnetic components. The intermediate frequency E-field signals are very impulsive, with some amplitude changes exceeding a factor of 100 in one measurement cycle. At low frequencies both the amplitudes and fluctuations are smaller. The high frequency band (1 O to 56 kHz) has a distinctly different temporal character, exhibiting very modest amplitude variations. The persistent "ripple" in the 17.8 kHz amplitudes occurs at approximately twice the spin-frequency (= 0.33 Hz) of ISEE-3, and indicates that this emission is polarized (see Section 5 below).

Rapid temporal variability is characteristic of the E-field waves downstream of the nose region bow shock, with the broadband "spikes" [Anderson et al., 1982] and "festoons" [Gallagher, 1985] being two conspicuous examples. The ISEE-3 wave instrument may not be capable of detecting spikes if their duration is less than the 8 msec inferred by Anderson, et al, [1982]; the AGC rise time of the ISEE-3 digital channels is at about 10 times longer than 8 msec. However, in the ISEE- 1 f-t wideband displays, the spikes appear to persist much longer than 8 msec; also, the spikes are detected in the I SEE- 1 digital channel measurements whose electronics are similar to those of the ISEE-3 wave instrument. Thus the impulsive E-field emissions measured downstream of the weak flank shocks could be of the same temporal character as the spiky waves detected by Anderson, et al. [1982] in the nose magnetosheath region.

For plasma conditions in the distant flank magnetosheath, the ISEE-3 wave instrument can be affected by the festoon-type modulation. The ISEE-3 antenna is L = 90 m (tip-to-tip), which is only somewhat smaller than the L = 215 m ISEE 1 antenna. For a linearly polarized electrostatic

wave with wave vector $k_\perp$ projected on the plane of the rotating antenna, the average potential across the antenna is given by Gallagher [1985].

$$\bar{\phi}(\psi) = \frac{\phi}{4} \frac{\mathrm{Sin}^2 x}{|x|}$$

where $x = (k_\perp L/4) \cos \psi$ involves the angle ψ between $K_\perp$ and the antenna, and ϕ is the wave potential amplitude. When $k_\perp L/4 << 1$, $\$ (\psi)$ is only weakly modulated, $\phi \propto \cos \psi$; since the ISEE-3 detector samples the potential at 60° intervals of rotation phase, we would expect variations in $\phi(\psi)$ to be typically in the range 2 to 4. For $k_\perp L/4 \geq \pi, \phi(\psi)$ has nulls in addition to the orthogonality nulls at $\psi = \pi/2, 3\pi/2$, and a strong maximum at tan x = 2x or x = 1.16; even for $k_\perp L/4 \leq \pi, \phi(\psi)$ has a modulation which is much larger than the variation of $\cos \psi$ for $0 < \psi \leq$ 80".

The plasma conditions downstream of the 1706 UT (0620 UT) flank shock produce an electron Debye length of λ_D = 610 cm (780 cm) which corresponds to $K_\perp L/4 = 2.9\, k_\perp \lambda_D$ (3.'7 $k_\perp \lambda_D$). Thus, linearly polarized waves with $k_\perp \lambda_D$ - 1 are subject to festoon modulation. A close examination of Figures 5 and 6 reveals intervals when the E-field amplitudes are strongly modulated at twice the satellite spin frequency; eg, near 1704 UT in the 1.0, 1.78, and 3.1 kHz channels, 1703:40-1704:00 in the 178 Hz channel, and throughout most of the 0621:30-0623:00 UT period in the low and mid-frequency channels. A strong festoon modulation ($kL/4 = \pi$) pattern consists of 2 large peaks symmetric about ψ = 90° per half spin period; however, the two peaks are separated by less than 60° in rotation phase (one 0.5 sec sampling interval), and thus could be detected as a single maximum by the ISEE-3 wave instrument. In addition to spin ripple, the strongest evidence that the ISEE-3 measurements are affected by the festoon modulation is that adjacent maximum and minimum amplitudes typically differ by factors of 10 to 100, which is much larger than would be expected for a simple cos ψ modulation but could be produced by the festoon effect when $kL/4 = \pi$.

Clearly the ISEE-3 wave instrument cannot definitively determine whether festoon modulation is affecting the measured amplitudes, and/or whether the observed variability results

fromimpulsive spikes. Experience from the nose region magnetosheath suggests that both should be present downstream of the flank shocks. If the festoon effect is important, we would conclude that the wavelength of the emissions in the frequency band from 200 Hz to 3 kHz (the same range identified by Gallagher, 1985) is of order $0.5 < k\lambda_D \leq 1$ or even somewhat higher. However, careful visual inspection of the ISEE- 1 digital channel measurements at 0.25 sec resolution presented by Anderson et al. [1982] casts some doubt as to whether the ISEE-3 data contains either spikes or festoons. In the ISEE- 1 data, spikes appear as simultaneous emissions from 1.0to31 kHz; the ISEE-3 impulsive signals do not extend across such a broad frequency range. The response of the ISEE- 1 channels to festoon modulation is a constant or slowly varying amplitude, in striking contrast to the large mid-frequency amplitude variations observed in the ISEE-3 data. Thus a possible, and perhaps the most reasonable, conclusion is that the observed ISEE-3 amplitude variations result from rotational modpolarized emission combined with intrinsic temporal variability of the wave amplitudes.

4.0 Electric Field Spectra - Averages and Comparisons

In this section we focus on the average spectral characteristics of the intermediate to low frequency magnetosheath emissions and compare the downstream regions of the flank and nose bow shocks. Figure 7 displays one-minute average and peak spectra for the two quasi-parallel and quasi-perpendicular shocks which we discussed in the last section. The two quasi-parallel average spectra exhibit a plateau from 100 Hz to 1.78 kHz at an amplitude of 2 x 10-5 V/m - $(Hz)^{1/2}$; the plateau passes through both the electron cyclotron and ion plasma frequencies. Above the ion plasma frequency, the spectrum falls monotonically; however, a weak upward inflection in the slope is apparent near the maximum Doppler shift frequency, which indicates the existence of the high frequency mode between the ion and electron plasma frequencies.

The spectra of the two quasi-perpendicular shocks appear different. A very well-defined spectral peak occurs near 1.78 to 3.16 kHz or roughly 2 to 5 times the ion plasma frequency, and a deep minimum exists between 100 Hz and 300 Hz. Since the average (and peak) amplitudes and spectral shape from 1-30 kHz are similar for the quasi-parallel and quasi-perpendicular shocks, the

relatively stronger (weaker) emission at 100 Hz to 300 Hz in the quasi-parallel (quasi-perpendicular) shock is responsible for the plateau (valley) shape of the spectra. At high frequencies, the quasi-perpendicular spectra also exhibit an upward inflection near the maximum Doppler frequency.

Figure 8 displays four magnetosheath spectra obtained by different spacecraft near the nose region of the bow shock. The one-minute average peak spectrum in 8a was measured by the ISEE-3 wave instrument on October 1, 1983, shortly after crossing an Alfven Mach number 11.7, θ_{Bn} = 72' shock. The broad 31 Hz to 560 Hz spectral plateau or gentle bump and the steep fall-off above the ion plasma frequency are typical of the spectra measured in strong shocks [Gurnett, 1985]. Figure 8b and 8c show two magnetosheath spectra measured by Rodriguez [1979] with IMP-6; the lower (upper) curve is a 5.6-minute average (0.1 second accumulation). The IMP-6 spectrum in Figure 8b was measured in the dawnside sheath at 60" to the sun-line. The low frequency portion of the peak spectrum in Figure 8a and 8b are nearly identical. In the range $f_{pi} \leq f \leq f_{pe}$, the IMP-6 spectrum has a slight bump or upward inflection which resembles the enhanced high frequency emission observed downstream of the flank shocks.

Figure 8d shows a nose region magnetosheath spectrum measured by the AMPTE wave SFR receiver [Onsager et al., 1989] downstream of an MA = 7, (l_{Bn} = 86" shock; to obtain Figure 8d, we have sampled the continuous SFR spectrum at the ISEE-3 logarithmically-spaced channels. The AMPTE and the Figure 8C IMP-6 spectra exhibit clear peaks of 1.0 kHz and 1.78 kHz, respectively, and the fall-offs in amplitude with frequency are similar. The AMPTE spectrum was measured in the dawnside sheath at 72" to the sun-line; the IMP-6 spectrum was also obtained on the dawnside but at about 20 R_E downstream of the terminator.

In comparing the spectra in Figures 7 and 8, the most striking relations between the flank and nose region emissions are: 1) the absence of the intense low frequency (30-300 Hz) "shock-like" component in the flank spectra; and 2) the strength of the intermediate frequency (1 -3 kHz) emissions on the flank is comparable to those in the nose region. At 1 kHz, Rodriguez [1979] found typical peak (O. 1 see) amplitudes of 10-4 to 10-5 V/m - $\sqrt{Hz}$, and a 5.46-minute average

amplitudes of 10-6 to 2 x 10^{-7} v/m - $\sqrt{Hz}$; amplitudes at these nose region levels are clearly present behind the lower Mach number flank shocks. In a statistical analysis of the AMPTE measurements, Onsager et al. [1989] found that the integrated wave energy density in the 0.2 kHz to 4 kHz band normalized to the electron pressure ($W = E^2/8\pi nT_e$) was W <10-10 for both quasi-perpendicular and quasi-parallel shocks with $M_A > 5$. The quasi-parallel flank shocks in Figure 7b have W $\approx 10^{-9}$, and the two quasi-perpendicular shocks have W = 2 x 10-9 (0528 UT) and W = 3 x 10^{-10} (05 15 UT). Hence, in both absolute wave intensity and normalized wave energy density, the flank magnetosheath waves are just as powerful as those which are observed in the nose region magnetosheath downstream of a significantly stronger bow shock.

5.0 Electric Field Polarization

The published reports on the electric field polarization of the nose region magnetosheath emissions are not entire] y consistent. Rodriguez [1979] concluded that the E-field was predominately parallel to the magnetic field. Anderson et al. [1982] found that the strongest spikes were polarized along the flow direction and that weaker spikes were field-aligned; for the festoon emissions, they reported perpendicular (parallel) polarization at ≥ 2 kHz ($\leq$ 2 kHz) frequencies. Gallagher [1985] states that although the festoon modulation requires a highly polarized wave, the electric field orientation had no relation to either the flow velocity or magnetic field directions. Finally, Onsager et al. [1989] state that the magnetosheath waves are polarized along the magnetic field.

Figure 9 displays the electric field polarization for the interval 0621:00 to 0622:30 UT downstream of the 0620 UT shock on September 23, 1983. In these polar representations, the radial distance is proportional to the logarithm (base 10) of the electric field spectral amplitude with a range of five decades from the center to the edge; the polar angle is measured from earth-sun line with the sun to the right. The lines at 35” and 2 15“ mark the ecliptic projection of the downstream magnetic field; the field inclination was only 9“ with respect to the ecliptic plane (the plane of the ISEE-3 antenna). From Figure 6, the magnetic field was very steady in direction and magnitude during the 90-second interval of polarization samples in Figure 9.

In the three lowest frequency channels, 178 Hz, 316 Hz; 1.0 kHz, the highest electric field amplitudes clearly have a tendency to occur when the antenna is oriented parallel to the magnetic field. At mid-frequencies (1 .78,3.16, and 5.67 kHz), the electric field does not exhibit a clear polarization, although the 1.78 kHz channel could be weakly polarized. Since the solar wind flow behind the weak quasi-perpendicular shock remains directed along the earth-sun line, i.e., almost the magnetic field direction, the absence of a clear mid-frequency polarization also implies that the waves are not polarized along the flow direction, In the two high frequency channels (10 and 17.8 kHz), the electric field is clearly polarized along the magnetic field; the coherent polarization at these frequencies supports the earlier conclusion based on spectral properties that this band represents a separate emission,

Figure 10 presents the electric field polarization measurements obtained between 1703:30 and 1705:00 UT downstream of the September 22, 1983, 1706 UT quasi-parallel shock. From Figures 1 and 5, during this period the x and z. components of the magnetic field underwent large oscillations. Given this level of magnetic turbulence, it is, perhaps, not surprising that none of the frequency channels exhibit even a mild tendency toward a preferred polarization direction. Since the solar wind flow velocity is little affected by the magnetic turbulence, the absence of a polarization along the earth-sun line strongly suggests that the waves are not polarized along the plasma flow direction.

6.0 Discussion

The electric field turbulence just downstream of the bow shock on the distant flank of the magnetosphere is quite similar in both wave amplitude and spectral character to the waves observed in the nose region magnetosheath behind a much stronger shock. The average E-field spectra generated by the low Mach number quasi-perpendicular shocks exhibits a strong mid-frequency peak which occurs just above the ion plasma frequency but well below the maximum Doppler shift frequency. The average downstream quasi-parallel wave spectra are plateau-shaped due to a low frequency (100-300 Hz) emission which is absent behind quasi-perpendicular shocks; from 1-30 kHz, the spectra are similar for both types of shocks. However, in contrast to the nose shock

region, the average spectra of the flank shocks do not show a low frequency peak--the shock-like spectrum of Rodriguez [1979] --although single sweep spectra occasionally exhibit a dominant low frequency emission. Both the absolute and the normalized E-field amplitudes produced by the high Mach number nose and low Mach number flank shocks are comparable. The very steady magnetic field downstream of the weak quasi-perpendicular shocks provided an ideal opportunity to measure the E-field polarization, a somewhat uncertain property of the nose magnetosheath waves. The emissions from 178 Hz to 1.0 kHz are clearly polarized along the magnetic field direction, which, for the shocks examined, is also the flow velocity direction. Near the 1.78 kHz -3.11 kHz spectral peak, the emissions do not show a dominant polarization. The E-field signals downstream of the flank quasi-parallel shock did not exhibit a polarization at any frequency, perhaps a consequence of the very turbulent magnetic field direction.

At high frequencies (10 kHz -30 kHz), we have identified a separate wave emission by a clear peak in higher time resolution spectra and a distinct inflection in the slope of the average spectra. This high frequency component occurs above the maximum Doppler shift frequency for $k\lambda_D = 1$, but below the electron plasma frequency and is clearly polarized parallel to the magnetic field behind the quasi-perpendicular shocks. For the nose magnetosheath waves, Onsager et al. [1989] emphasized the occurrence of emissions above the maximum Doppler shift frequency but did not identify this high frequency band as a separate emission as distinguished from a smooth continuation of the high frequency tail of the mid-frequency peak.

At high time resolution, the low and mid-frequency E-field waves exhibit rapid temporal vanability with amplitude fluctuations of 10 to 100; the high frequency component varies by factors of 2 to 4. The amplitude variations often are modulated at twice the ISEE-3 spin frequency. The most straightforward interpretation of this spin-ripple is that the wave E-fields are coherently polarized on time scales of several satellite rotations. The low and high frequency components do exhibit a well defined polarization direction, and their relative low to modest amplitude fluctuations could be consistent with a simple cosine projection of the electric field on the antenna. The mid-frequency signals do not exhibit a clear polarization, although the large amplitude fluctuations

could render a polarization undetectable in the ISEE-3 data. We discussed the possibility that festoon modulation might be responsible for the amplitude variations, but, based on a visual comparison with the ISEE-1 channel measurements of festoons, we believe that this explanation is unlikely. Furthermore, in the distant geomagnetic tail, the ISEE-3 wave detector has measured rapidly varying signal amplitudes in the low and mid-frequency channels in plasmas where the very long Debye length precludes festoon modulation; these highly impulsive signals also often appear to be modulated at twice the satellite spin-frequency. Thus we conclude that the mid-frequency emissions downstream of the flank shocks are probably intrinsically highly impulsive.

The origin of these shock associated emission is at present unknown. Onsager, et al's [1989] suggestion that cool electron beams can excite waves with $f>f_D$ might explain the high frequency wave component if the electron beam speed is comparable to the background electron thermal speed. The well defined parallel polarization of these emissions argues in favor of an unstable mode ongin. Onsager, et. al., [1989] suggest that the cold electron beams might be formed by a "time-of-flight" mechanism, as occurs in the foreshock region [Filbert and Kellogg, 1979]; spatial and temporal discontinuities in the shock structure would accelerate cold electron beams that traveled downstream, or stable enhanced super-thermal tails at the shock overtake downstream electrons with suppressed tails to create locally unstable distributions.

Here we suggest that the high frequency waves are generated by a variation of the "time-of-flight" mechanism which involves the low energy part of the electron distribution. In crossing a fast, non-perpendicular shock upstream electrons are accelerated downstream by the cross-shock potential electric field and decelerated by the parallel magnetic gradient force [Feldman, 1985; Scudder, et. al., 1986]. If the electron motion through the shock were strictly adiabatic, a large void would develop in the low energy electron distribution, and the electron density would be insufficient to balance the compressed ion density. Thus the electron void must be rapidly filled by scattering upstream electrons into the void as they transit the shock [Veltri, et. al., 1990] and/or by populating the void's phase space region with downstream electrons that travel toward the shock. Although the detailed physical processes responsible for filling the void are still unclear, it is very

unlikely that the distribution of the electrons that fill the void will always match smoothly with the electron distribution outside of the void. Furthermore, temporal and spatial variability in the shock structure will induce fluctuations in the void boundaries and filling rates which w-ill propagate downstream and create local discontinuities in the electron distributions by the "time-of-flight" process.

As a simple model for a discontinuity in the distribution function, we model the reduced parallel electron distribution (after integrating over the perpendicular velocity) by

$$F(v_{11}) = f_1 H(u - v_{11}) + f_2 H(v_{11} - u) \qquad (1)$$

where f_1 (f_2) is Maxwellian with density n_1 (n_2) and temperature T_1 (T_2), and H(x) is the Heavyside step function. If $f_1(u) \neq f_2(u)$, $F(v_{11})$ has a discontinuity at the speed $V_{11}=u$. Substituting $F(v_{11})$ into the electrostatic dispersion relation for parallel propagating waves, and neglecting the ion contribution for waves with frequencies well-above the ion plasma frequency, the dielectric function can be written as [Coroniti, et. al., 1993]

$$\varepsilon = 1 + k^2 \lambda_D - \frac{\Delta \bar{a}}{u - \omega/k} + i\pi R \frac{\omega}{k\bar{a}} \qquad (2)$$

where λ_D is a slightly modified Debye length, and $\bar{a}^2 = (T_1 T_2/m^2)^{1/2}$. If $n_2 = n_1 + \delta n$, $T_2 = T_1 + \delta T$ with $\delta n/n_1 << 1$ and $\delta T/T_1 << 1$, the parameter A, which measures the discontinuity in $F(v_{11})$, is approximately

$$\Delta = \frac{\exp[-u^2/a_1^2]}{2\sqrt{\pi}} \left[\frac{\delta n}{n_1} - \frac{\delta T}{2T_1} + \frac{u^2}{a^2}\frac{\delta T}{T_1}\right] \qquad (3)$$

and $R = 1/\sqrt{\pi}$. In deriving (2), ω/k was assumed small compared to the thermal speed, and the nonresonant terms proportional to ω^2/k^2a^2 and higher were dropped.

For A <<1, the solution to&= O is the dispersion relation

$$\omega/k\bar{a} = \bar{u} - \frac{\Delta\,(1 + k^2\lambda_D^2)}{\left[\bar{a}^2 + \left(1 + k^2\lambda_D^2\right)^2\right]} + i\,\frac{\Delta\bar{u}}{\pi R\left[\bar{u}^2 + \dfrac{\left(1 + k^2\lambda_D^2\right)^2}{\pi^2 R^2}\right]} \qquad (4)$$

where ii = u/a. Thus if A > 0, the discontinuity excites a "beam-like" mode with real frequency (in the solar wind frame) $\omega_r \approx$ ku and growth rate $\gamma \sim \Delta\omega_r/\sqrt{\pi}$. The growth rate maximizes at $k^2\lambda_D^2 = -1/3 + [4/9 + \pi/3\,\bar{u}^2]^{1/2}$, so that waves should be excited up to wave number $k\lambda_D$ -1. In the spacecraft frame the wave frequencies can extend up to $f \sim k\lambda_D V_e$) fp_e which can be comparable to fp_e.

The instability should saturate when the effective trapping velocity $\frac{\omega_r}{k} \approx (eE/mk)^{1/2}$ becomes comparable to the difference between the discontinuity speed u and ω/k; electrons with $v_{11} \approx$ u will then be in Landan resonance with the excited waves and scattering by the wave electric field will smooth the discontinuity. Setting $\omega_r/k \sim$ aA (from (4)), we find the saturation electric field $E \sim (m/e)\,k\lambda_D\, a\, \omega_p\, \Delta^2$. For a frequency f- 10 kHz, and the typical downstream parameters of the flank shocks the, saturation amplitude is $E_v \cong E/\sqrt{f} \sim 3 \times 10^{-2}$ A² V/m -$\sqrt{\text{Hz}}$. Since the observed peak amplitudes, of the high frequency emission are -107 V/m-$\sqrt{\text{Hz}}$, we can estimate the discontinuity parameter as A - 10^{-3}. Thus only very small perturbations in the value of the local electron distribution function, but correspondingly large gradients in velocity space, may be required to generate the polarized high frequency waves.

Downstream of shocks, and presumably other large scale discontinuities and boundaries, the relaxation of the electron distribution to a smooth equilibrium state is prevented by the electron's rapid ballistic communication with the fluctuating shock structure. "Time-of-flight" effects continuously induce small local discontinuities in the distribution function which excite and are removed by a low level of electric field wave turbulence. Just how far downstream this wave turbulence extends is an open question, but the high electron thermal speed suggest that the relaxation region could be very large.

Finally, the identification and origin of the intermediate frequency emission remains uncertain. Rodriquez [1979] noted that the peaked spectral shape of the magnetosheath signals was similar to the so-called ion acoustic waves detected in the solar wind [Gurnett and Frank 1978] and in regions upstream of the quasi-parallel bow shock. Figure 11 compares a one minute average spectrum obtained downstream of the 0620 UT quasi-perpendicular flank shock and an upstream wave spectrum measured by ISEE-2 [Anderson etal, 1981]; clearly the peak and one-minute average upstream and downstream spectra are nearly identical. Anderson, et al [1981] Eastman, et al [198 1], and Parks, et al [1981] demonstrate that the upstream mid-frequency emissions are closely associated with enhanced fluxes of escaping ions which maybe non-gyrotropic and bunched in physical space. Using wideband measurements, Anderson, et al [1981] showed that the broad spectral peak resulted from frequent, rapid (10-20 see) sweeping of the center frequency of a relative] y narrow band (~ 1 kHz) emission over a range from 1 to 10 kHz. Since 10 kHz was near the maximum Doppler shift frequency for $k\lambda_D \approx 1$, they interpreted the mid-frequency emission as parallel propagating ion acoustic waves with a variable Doppler shift frequency due to changes in the magnetic field direction, However, from a festion modulation analysis Fusilier and Gurnett [1984] found that the upstream waves propagated at 40° $\pm$ 20° to the magnetic field rather than parallel. Furthermore the magnetic field variations measured during several of Anderson, et al's sweeping events are inconsistent with a Doppler shift interpretation of the observed frequency changes if k is parallel to B.

In the absence of wideband measurements we cannot determine whether the downstream mid-frequency emissions have a sweeping frequency character, although the similarity of the downstream and upstream spectra suggest this possibility. If the downstream waves are intrinsically narrowbanded with a variable center frequency, the frequency sweeping cannot be due to magnetic field fluctuations since the field downstream of the weak quasi-perpendicular shocks was very steady. If in addition, the downstream waves are associated with suprathermal ion fluxes, possibly with non-gyrotropic distributions, then even weak shocks, must be capable of accelerating ions to several times the solar wind speed.

Acknowledgements. This work was supported at TRW by NASA contract NAS5-31837 (FVC), NASW-4749 (EWG) and NAS5-31216 (SLM). The work at the California Institute of Technology, Jet Propulsion Laboratory was performed under contract with NASA.

References

Anderson, R. R., G. K. Parks, T. E. Eastman, D. A. Gurnett, and L. A. Frank, "Plasma Waves, Associated with Energetic Particles Streaming Into The Solar Wind From The Earth's Bow Shock", J. Geophys. Res., 86, 4493, 1981.

Anderson, R. R., C. C. Harvey, M. M. Hoppe, B. T. Tsurutani, T. E. Eastman, and J.Etcheto, "Plasma Waves Near The Magnetopause", J. Geophys. Res., 87, 2087, 1982.

Coroniti, F. V., M. Ashour-Abdalla, and R. R. Richard, "Electron Hole Mode Instability", J. Geophys. Res., submitted, 1993.

Eastman, T. E., R. R.Anderson, L. A.Frank, and G. K. Parks, "Upstream Particles Observed in The Earth's Foreshock Region", J. Geophys. Res., 86, 4379, 1981.

Etcheto, J., and M. Faucheux, "Detailed Study of Electron Plasma Waves Upstream of the Earth's Bow Shock", J. Geophys. Res., 89, 6631, 1984.

Feldman, W. C., "Electron Velocity Distribution Near Collisionless Shocks" in Collisionless S ocks in the Heliosphere: Review of Current Research Geophys. Memo Res., Vol. 35, edited by B. Tsurutani and R. G. Stone, pp. 195-205, AGU, Washington, D. C., 1985.

Filbert, P. C., and P. J. Kellogg, "Electrostatic Noise at the Plasma Frequency Beyond the Earth's Bow Shock", J. Geophys. Res., 84, 1369, 1979.

Fuselier, S. A., D. A. Gurnett, "Short Wavelength Ion Waves Upstream of the Earth's Low Shock", J. Geophys. Res., 89, 91, 1984.

Fuselier, S. A., D. A. Gurnett, and R. J. Fitzenreiter, "The Downshift of Electron Plasma Oscillations in the Electron Foreshock Region", J. Geophys. Res, 90, 3935, 1985.

Gallagher, D. L., "Short Wavelength Electrostatic Waves in the Earth's Magnetosheath", Ph.D. Dissertation, Univ. of Iowa, Iowa City, 1982.

Gallagher, D. L., "Short-Wavelength Electrostatic Waves in the Earth's Magnetosheath", J. Geophys. Res., 90, 1435, 1985.

Greenstadt, E. W., D. P. Traver, F. V. Coroniti, E. J. Smith, and J. R. Slavin, "Observations of the Flank of Earth's Bow Shock to 110 RE by ISEE3/ICE", Geophys. Rest Lett., 17, 753, 1990.

Gurnett, D. A., and L. A. Frank,''Ion Acoustic Waves in the Solar Wind", J. Geophys. Res., 83, 58, 1978.

Gurnett, D. A., "Plasma Waves and Instabilities" in Collisionless Shocks in the Heliosphere: Review of Current Research, Geophvs, Mono Ser., Vol. 35, edited by B. J. Trusutani and R. G. Stone, pp. 207-224, AGU, Washington, D. C., 1985.

Kennel, C. F., F. L. Scarf, F. V. Coroniti, E. J. Smith, and D. A. Gurnett, "Nonlocal Plasma Wave Turbulence Associated With Interplantary Shocks", J. Geophvs, Res., 87, 17, 1982.

Onsager, T. G., R. H. Holzworth, H. C. Koons, O. H. Bauer, D.A. Gurnett,

R. R. Anderson, H. Luhr, and C. W. Carlson, "High Frequency Electrostatic Waves Near Earth's Bow Shock", J Geophys. Res., 94,13, 39731989.

Parks, G. K., E. W. Greenstadt, C.S. Wu, A. St. Mark, R, P. Lin, K. A. Anderson, C. Gargiolo, B. Mauk, H. Reme, R.Anderson, and T. Eastman, "Upstream Particle Spatial Gradients and Plasma Waves", J. Geophys. Res., 86, 4343.1981.

Rodriguez, P., "Magnetosheath Electrostatic Turbulence", J. Geophys. Res., 84, 917, 1979.

Rodriguez, P., and D.A. Gurnett, "Electrostatic and Electromagnetic Turbulence Associated with the Earth's Bow Shock", J. Geophys. Res., 80, 19.1975.

Scudder, J. D., A. Mangeney, C. Lacombe, C. C. Harvey, C. S. Wu, and R. R. Anderson, "The Resolved Layer of a Collisionless, High β, Supercritical, Quasi-Perpendicular Shock Wave 3. Vlasov Electrodynamics", J. Geophys. Res., 91, 11,075, 1986.

Veltri, P., A. Mangeney, and J. D. Scudder, "Electron Heating in Quasi-Perpendicular Shocks", . Geophys. Res., 95, 14, 939, 1990.

Figure Captions

Figure 1: The quasi-parallel flank bow shock observed by ISEE-3 on September 22,1983. The top left panel shows the wave electric field spectral amplitude with a scale of five decades; the solid (single) curve is the 3-second average (peak in three-second intercals) and the channel frequencies range from 178 Hz to 56.2 KHz. The two lower left panels show the 3-second average magnitude (B_z) and Z-component (B_z) of the magnetic field The right panel displays selected electric field amplitude spectra from 10 Hz to 100 KHz. The two shock crossings occurred at 1706 and 1708 UT, and had shock normal angles of θ_{Bn} = 190.

Figure 2: The θ_{Bn} = 37° quasi-parallel bow shock observed by ISEE-3 at 1552 UT on September 22, 1983. The format is the same as in Figure 1. The numbers 1 and 2 refer to the times at which the two 3-second peak and average electric field amplitude spectra were obtained.

Figure 3: The θ_{Bn} = 62o quasi-perpendicular bow shock observed by ISEE-3 at 0515 UT on September 23, 1983. The format is the same as in Figure 1.

Figure 4: The θ_{Bn} = 72o quasi-perpendicular bow shock observed by ISEE-3 at 0528 UT on September 23, 1983. The format is similar to Figure 1 except that the X-component of the magnetic is displayed instead of the Z-component.

Figure 5: High time resolution measurements from 1703 to 1704:30 UT downstream of the September 22, 1983, quasi-parallel bow shock. The top four panels display the unaveraged, 1/6 second per vector, magnetic field components and magnitude. The bottom panels display the wave electric field spectral amplitudes at the highest resolution of 0.5 second per spectrum; the amplitude scale covers four orders of magnetude.

Figure 6: High time resolution measurements from 0621:30 to 0623:00 UT for the 0622 UT θ_{Bn} = 67o quasi-perpendicular shock observed by ISEE-3 on September 23, 1983. The format is the same as Figure 5. The shock ramp occurred at 0622:44 UT and was very sharp even in the high resolution magnetic field measurements. Although the upstream region contained significant high frequency magnetic fluctuations, the downstream field was very steady.

Figure 7: One minute peak (upper curve) and average (lower curve) electric field amplitude spectra for the two September 22, 1983 quasi-parallel shocks (top panels) and the two September 23, 1983 quasi-perpendicular shocks (bottom panels) f_{ce} denotes. the electron cyclotron frequency, fpi (f_w) denotes the ion (electron) plasma frequency, and f_D is the maximum Doppler shift frequency for waves with $k\lambda_D = 1$.

Figure 8: The upper left panel (a) is an one minute peak and average electric field amplitude spectrum obtained by ISEE-3 on October 1, 1983 downstream of a strong quasi-perpendicular bow shock which was crossed near the nose of the magnetosphere. Panels&b and 8c are magnetosheath electric field amplitude spectra measured by the IMP 6, and have been derived from the power spectra presented by Rodriquez (1979); the upper (lower) curve is the 0.1 second (5.6 minute average) spectrum. Panel 8d is the electric field amplitude spectra measured by the AMPTE swept frequency receives in the nose region magnetosheath; the spectrum was adopted from the measurements presented by On sager, et al. (1989).

Figure 9ab: Electric field wave polarization downstream of the September 23,19830622 UT quasi-perpendicular shock. The radial scale in each polar plot represents five orders of magnitude in spectral amplitude. Each point is the ecliptic plane component of the electric field spectral amplitude measured at the corresponding phase angle with the sun at the right. The line labeled B represents the projection of the magnetic field onto the rotational (ecliptic) plane of the ISEE-3 electric field antenna.

Figure 10ab: Electric field wave polarization downstream of the September 22,19831706 UT quasi-parallel shock. The format is the same as in Figure 9.

Figure 11: Comparison between the electric field amplitude spectrum measured by ISEE-3 downstream of the 0620 UT quasi-perpendicular flank bow shock (solid curve) and the spectrum measured by ISEE-2 in the region upstream of the nose region bow shock (dashed curve). The upstream spectrum is adapted from a spectrum shown by Anderson, et. al (1981).

[SE E-3 Sept. 22, 1983

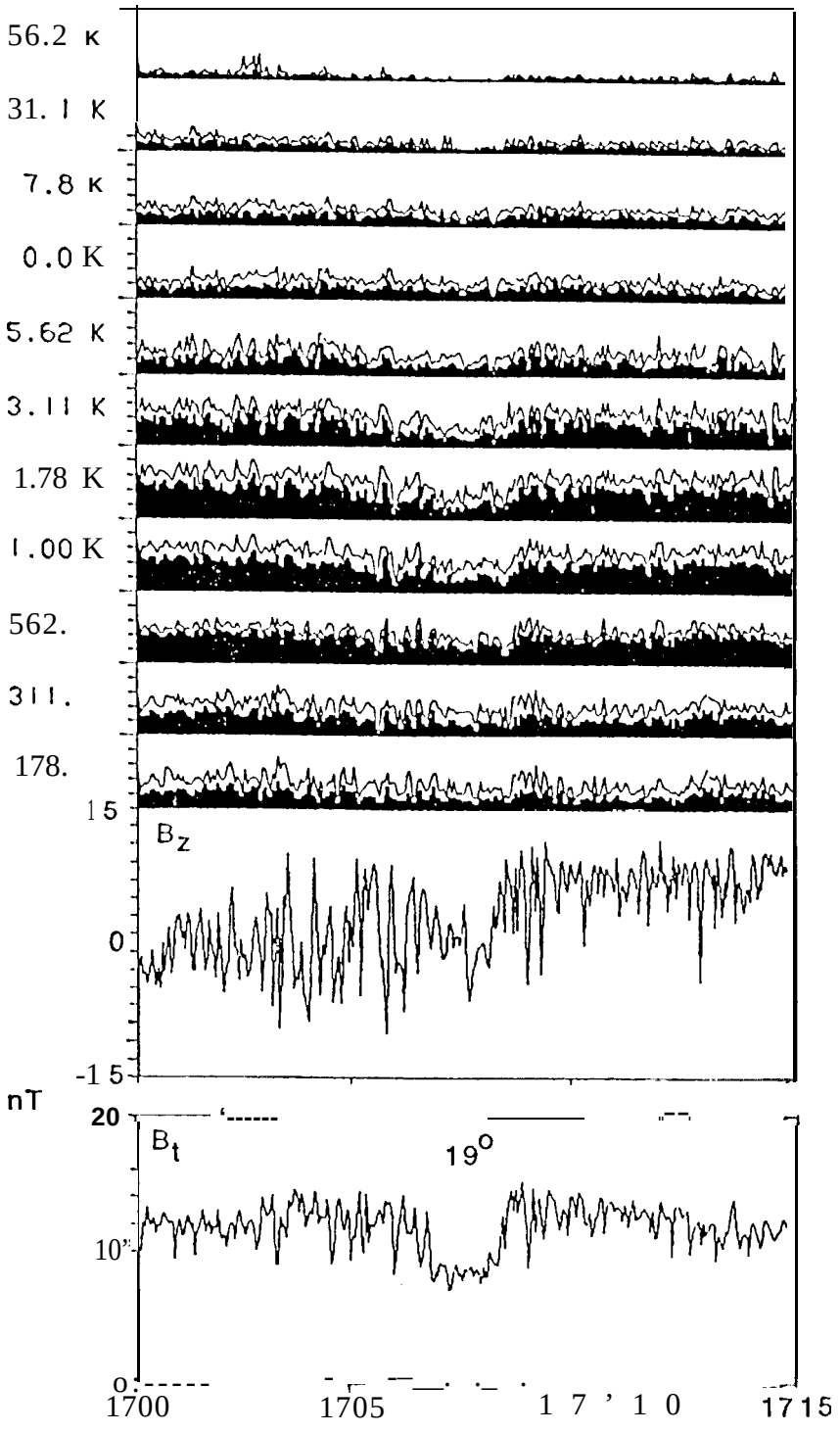

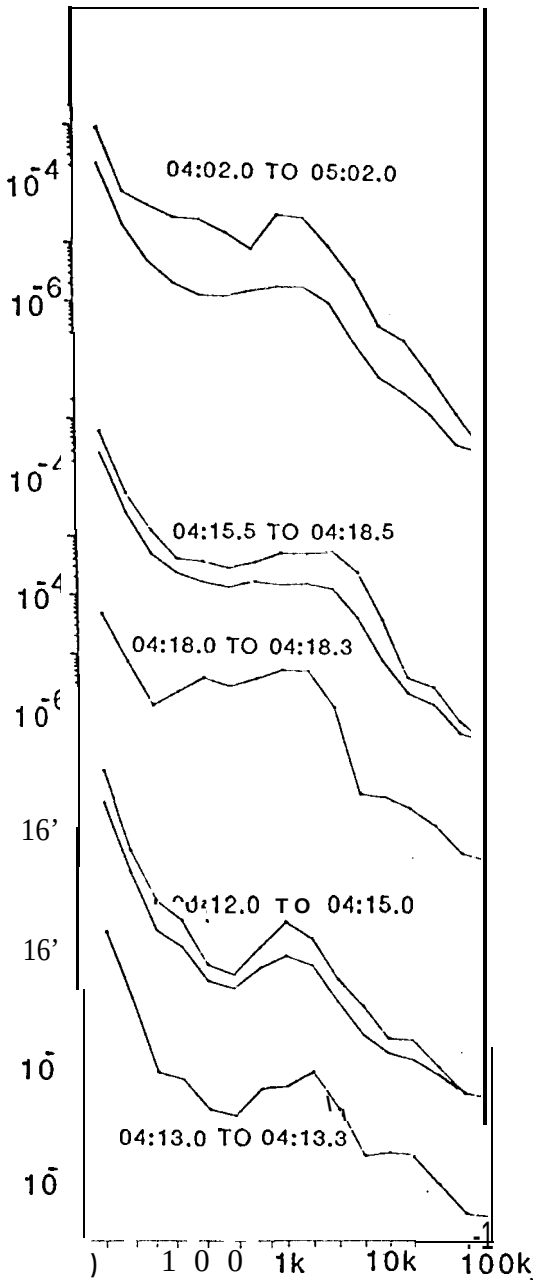

FIG. 1

ISEE 3 Sept. 22, 1983

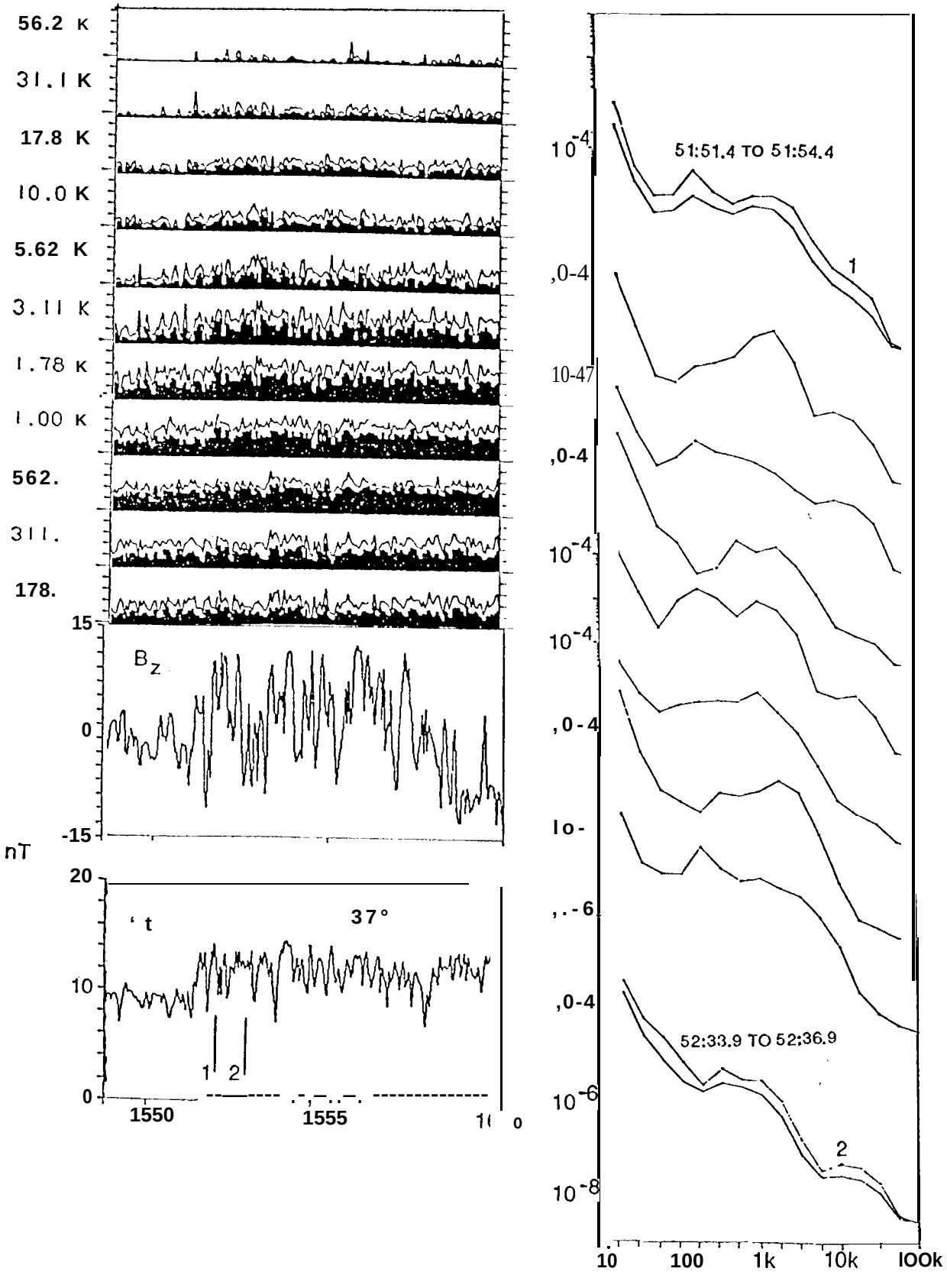

FIG. 2.

ISEE-3 Sept. 23, 1983

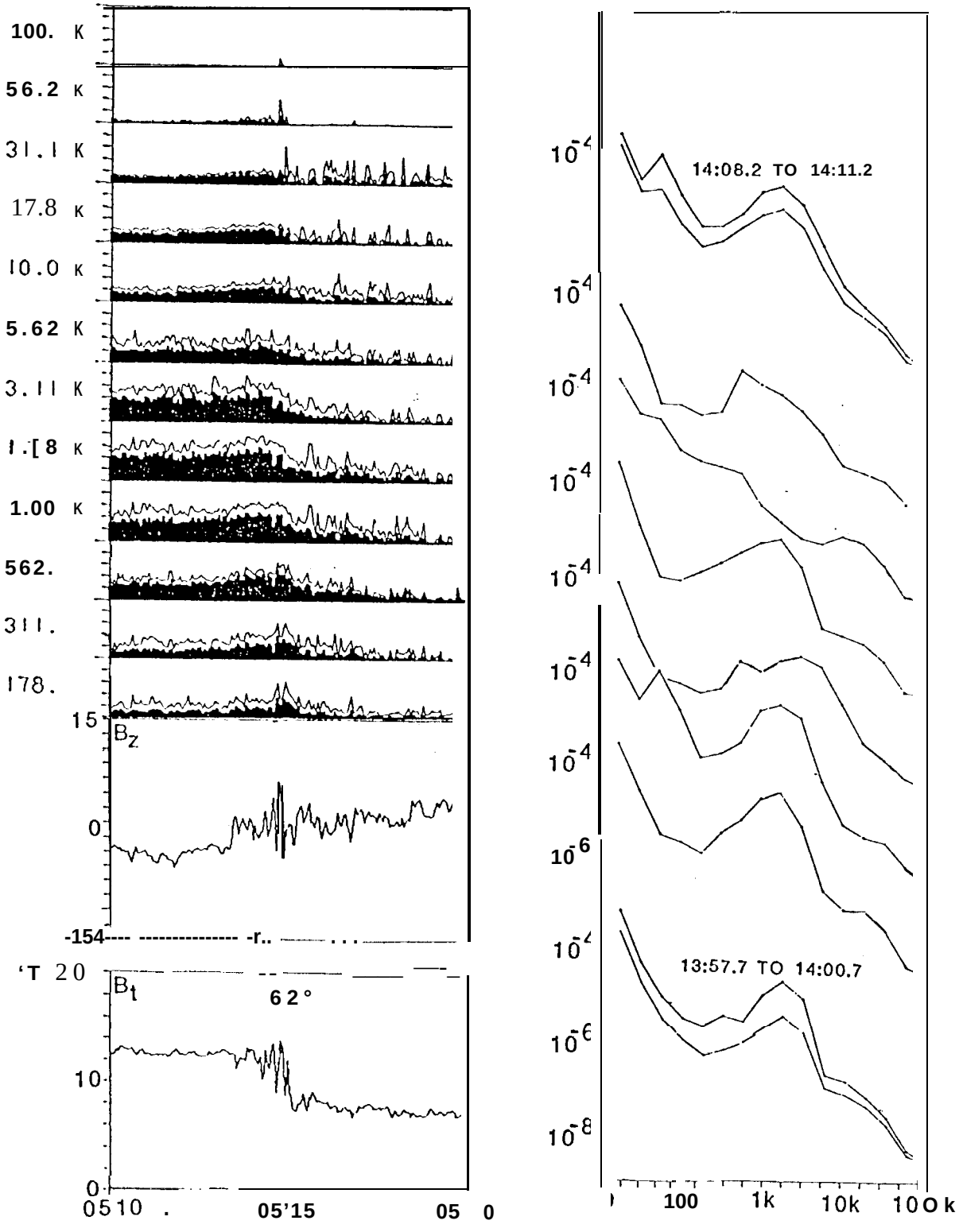

F16.3

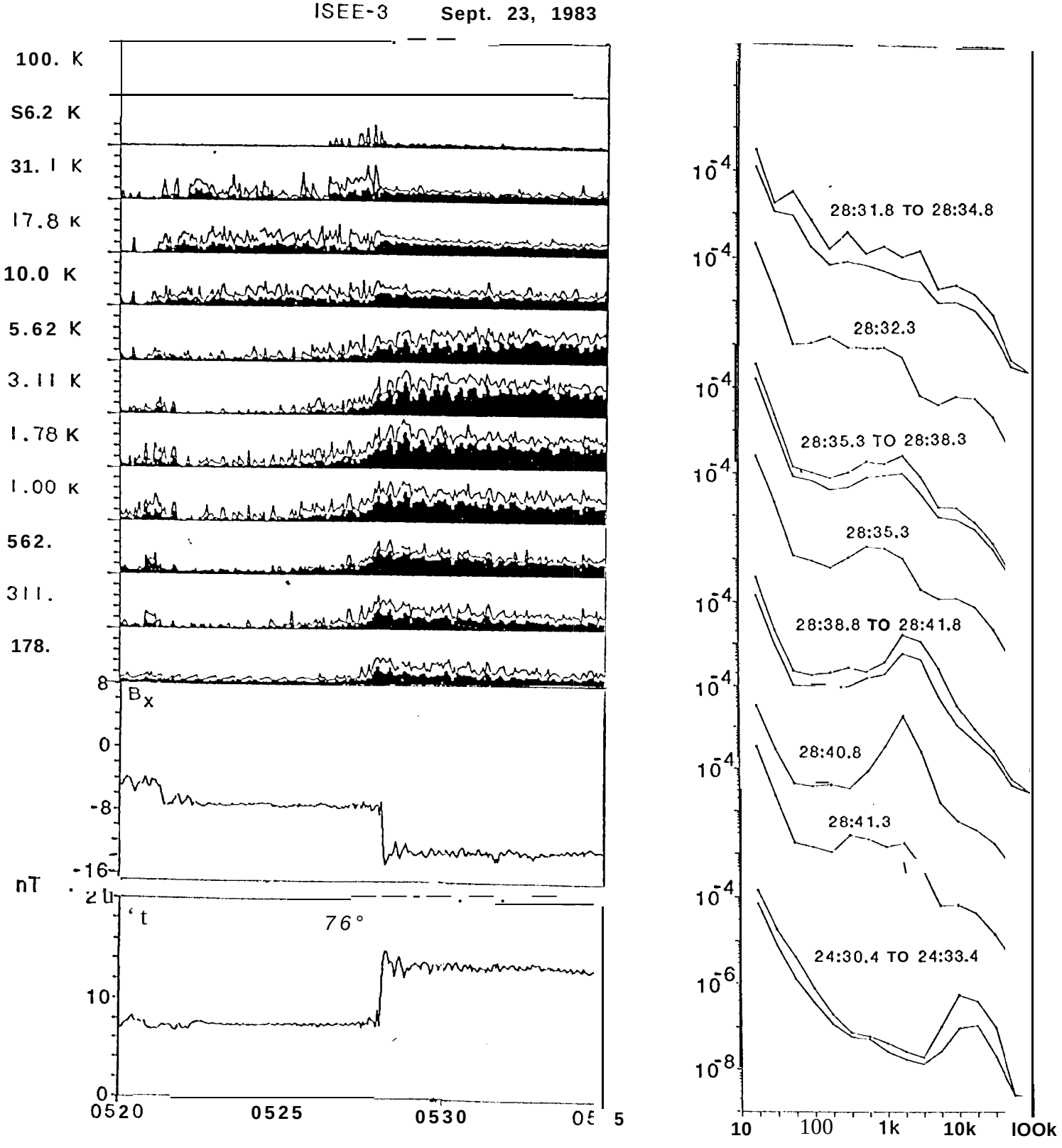
ISEE-3 Sept. 23, 1983
100. K
S6.2 K
31. I K
17.8 K
10.0 K
5.62 K
3.11 K
1.78 K
1.00 K
562.
311.
178.
8
B_x
0
-8
-16
nT
76°
10
0
0520
0525
0530
10^-4
10^-6
10^-8
28:31.8 TO 28:34.8
28:32.3
28:35.3 TO 28:38.3
28:35.3
28:38.8 TO 28:41.8
28:40.8
28:41.3
24:30.4 TO 24:33.4
10
100
1k
10k
IOOk

FIG. 4

ISEE-3 Sept. 22, 1983

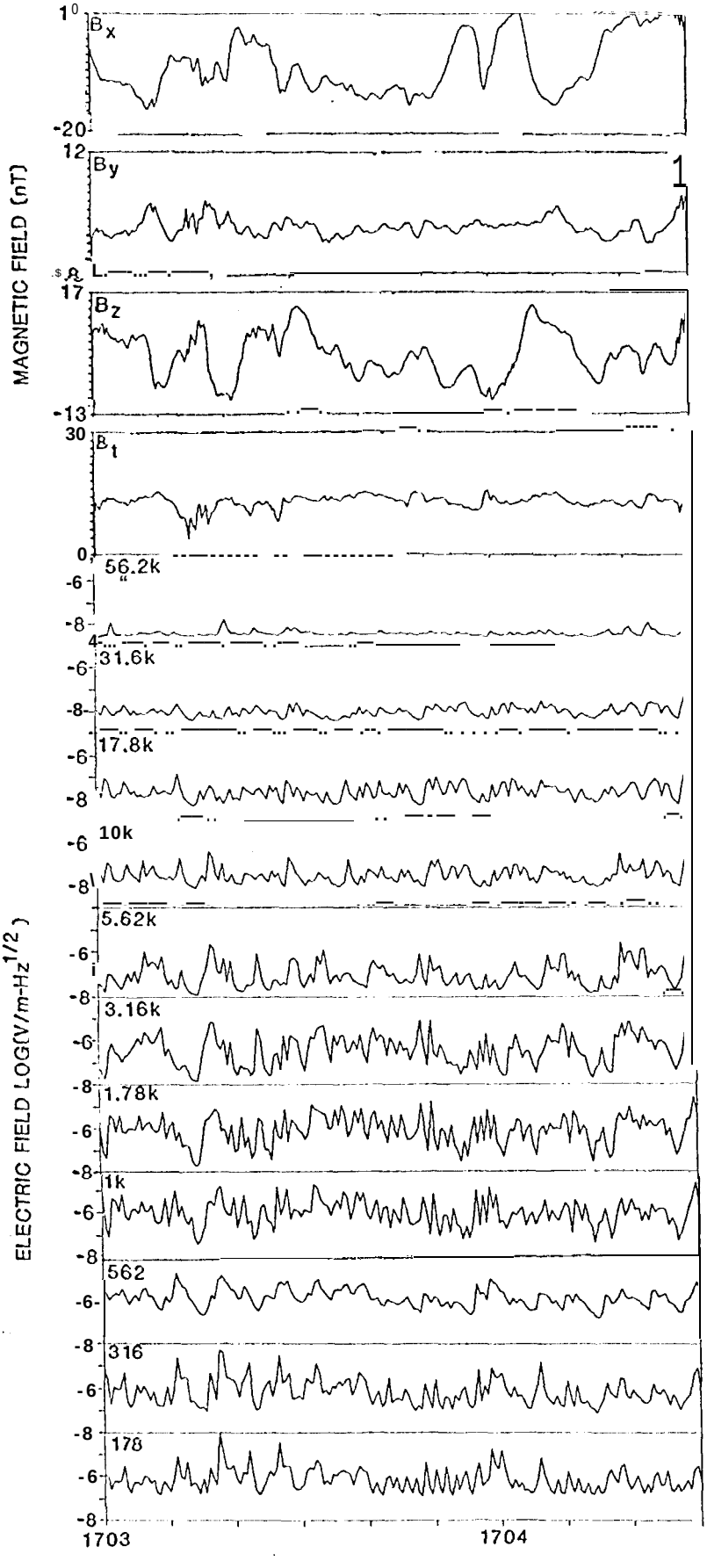

Fig. 5

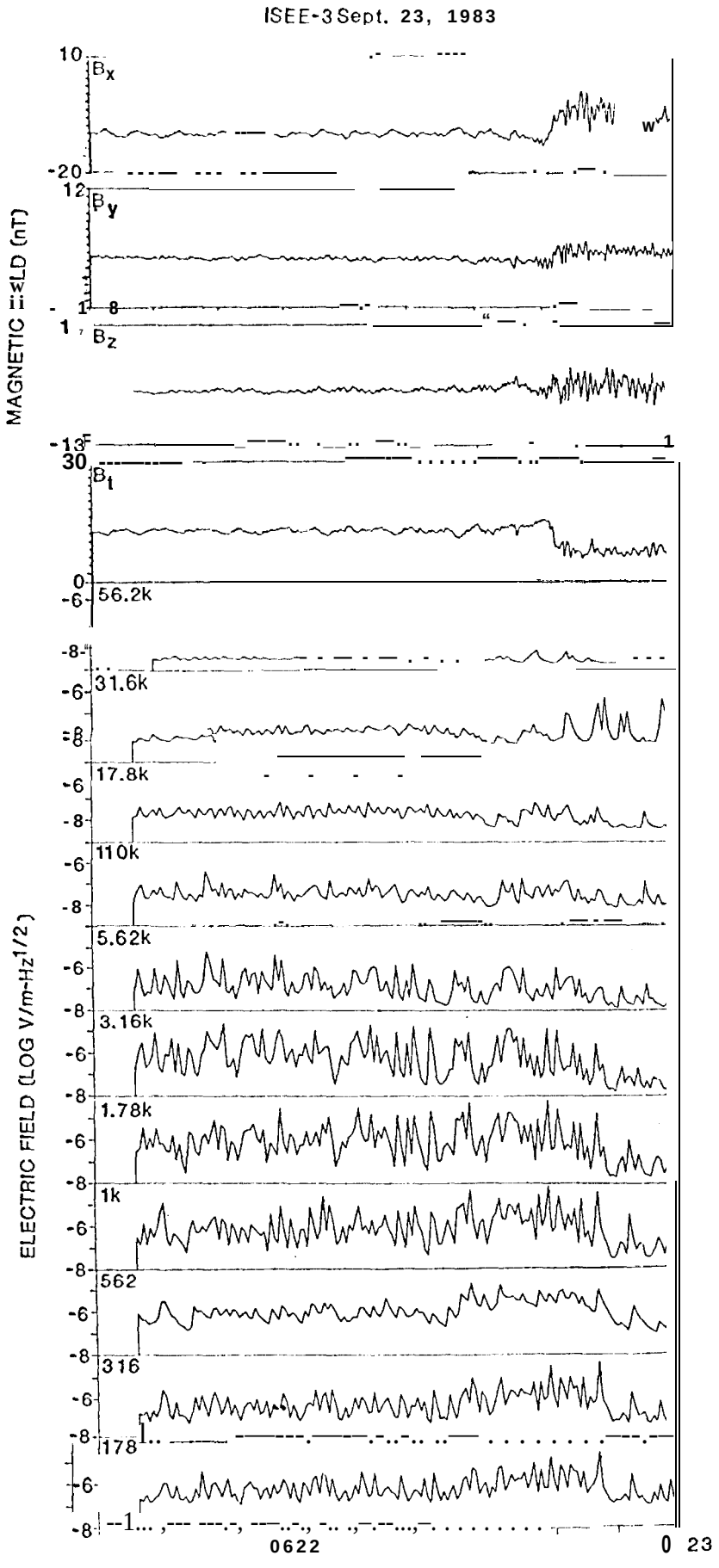
ISEE-3 Sept. 23, 1983
MAGNETIC FIELD (nT)
10
-20
B_x
12
B_y
1
B_z
-13
30
B_t
0
-6
56.2k
31.6k
17.8k
110k
5.62k
3.16k
1.78k
1k
562
316
178
ELECTRIC FIELD (LOG V/m-Hz$^{1/2}$)
0622
0 23

Fig. 6

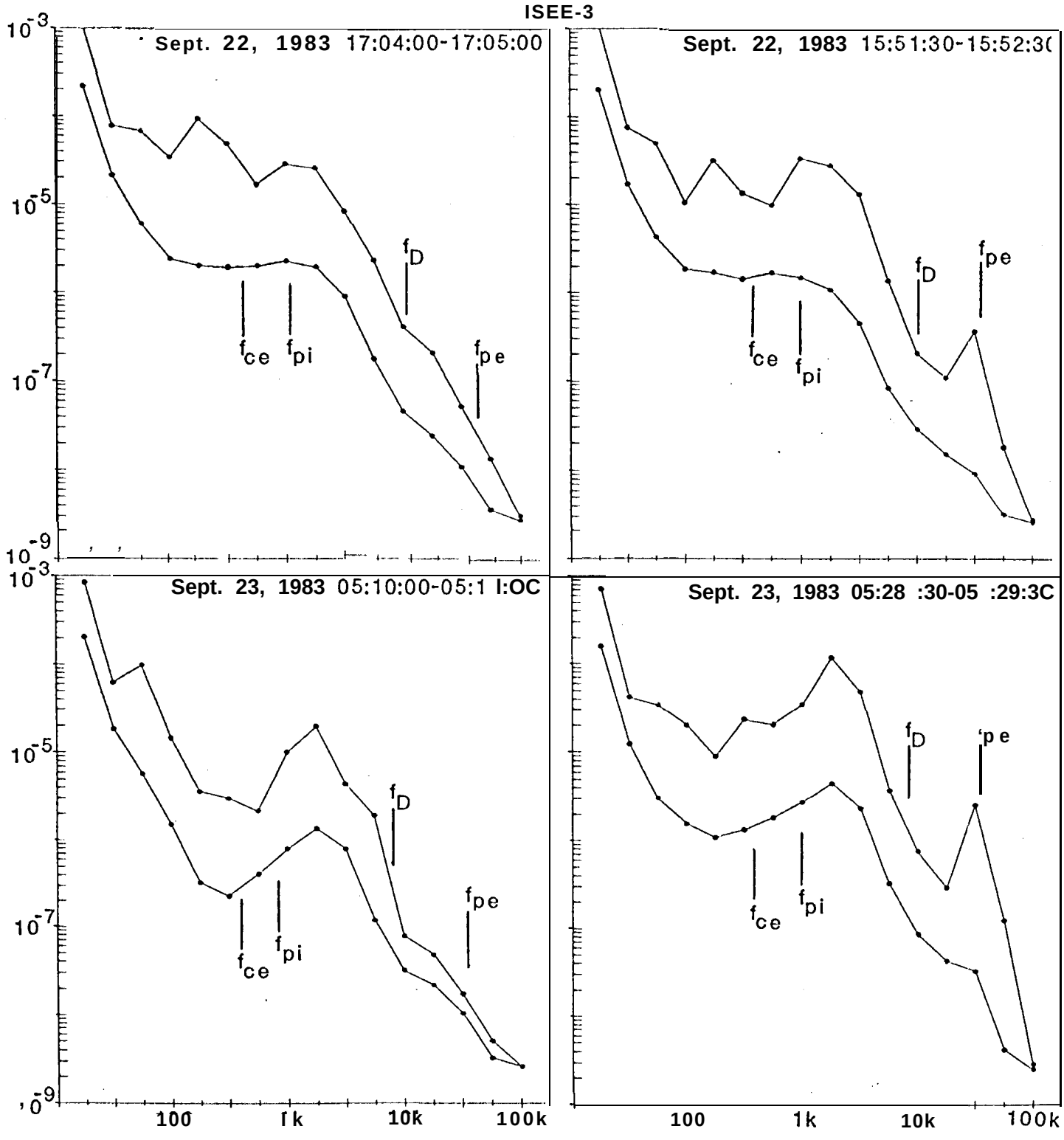
ISEE-3
Sept. 22, 1983 17:04:00-17:05:00
Sept. 22, 1983 15:51:30-15:52:30
Sept. 23, 1983 05:10:00-05:11:OC
Sept. 23, 1983 05:28 :30-05 :29:3C
10^{-3}
10^{-5}
10^{-7}
10^{-9}
f_D
f_{ce}
f_{pi}
f_{pe}
100
1k
10k
100k

Fig.7

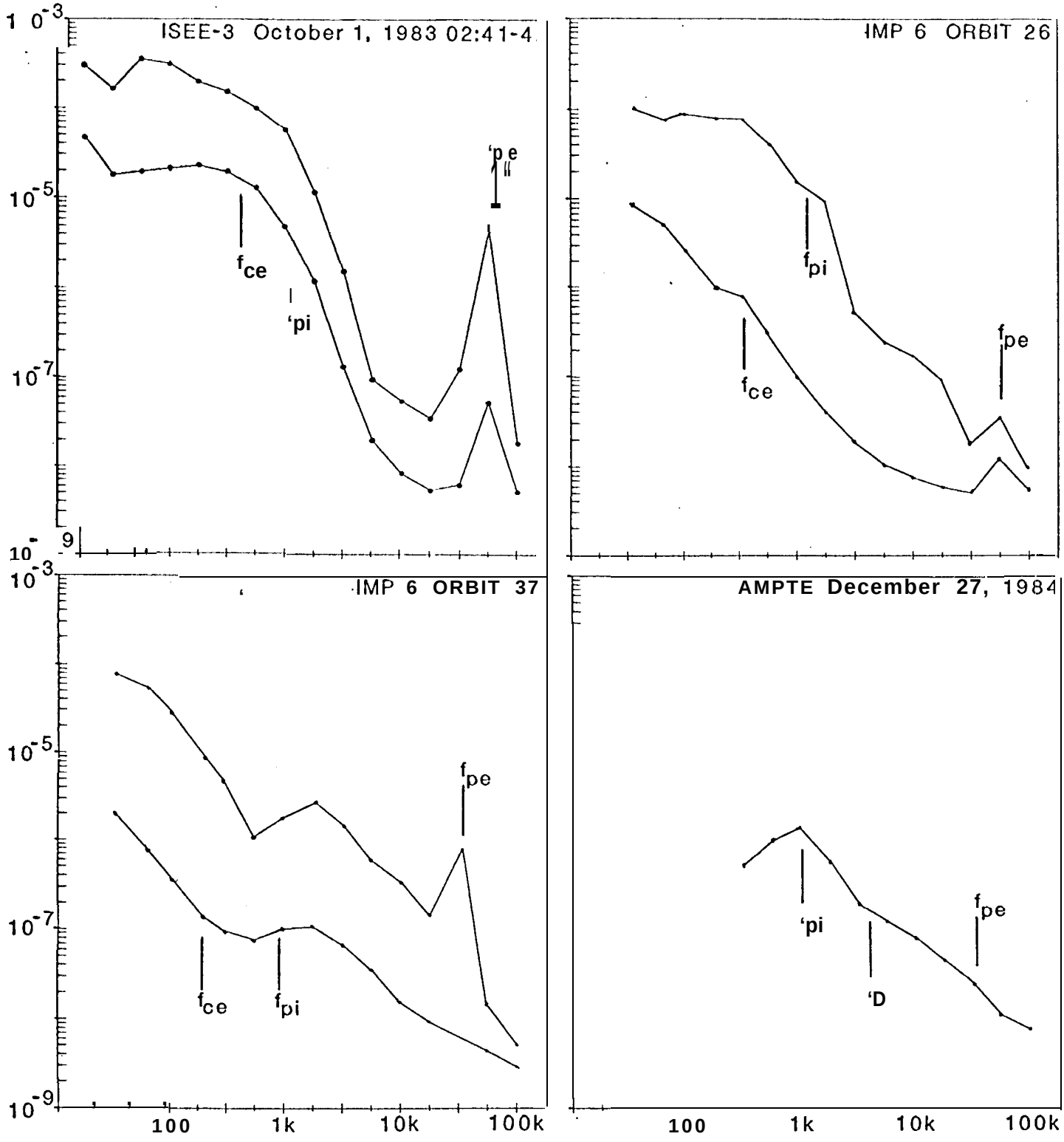
ISEE-3 October 1, 1983 02:41-4
IMP 6 ORBIT 26
IMP 6 ORBIT 37
AMPTE December 27, 1984
1 0^-3
10^-5
10^-7
10^-9
f_ce
f_pi
f_pe
100
1k
10k
100k

Fig. 8

ISEE-3 September 23, 19836:21:00

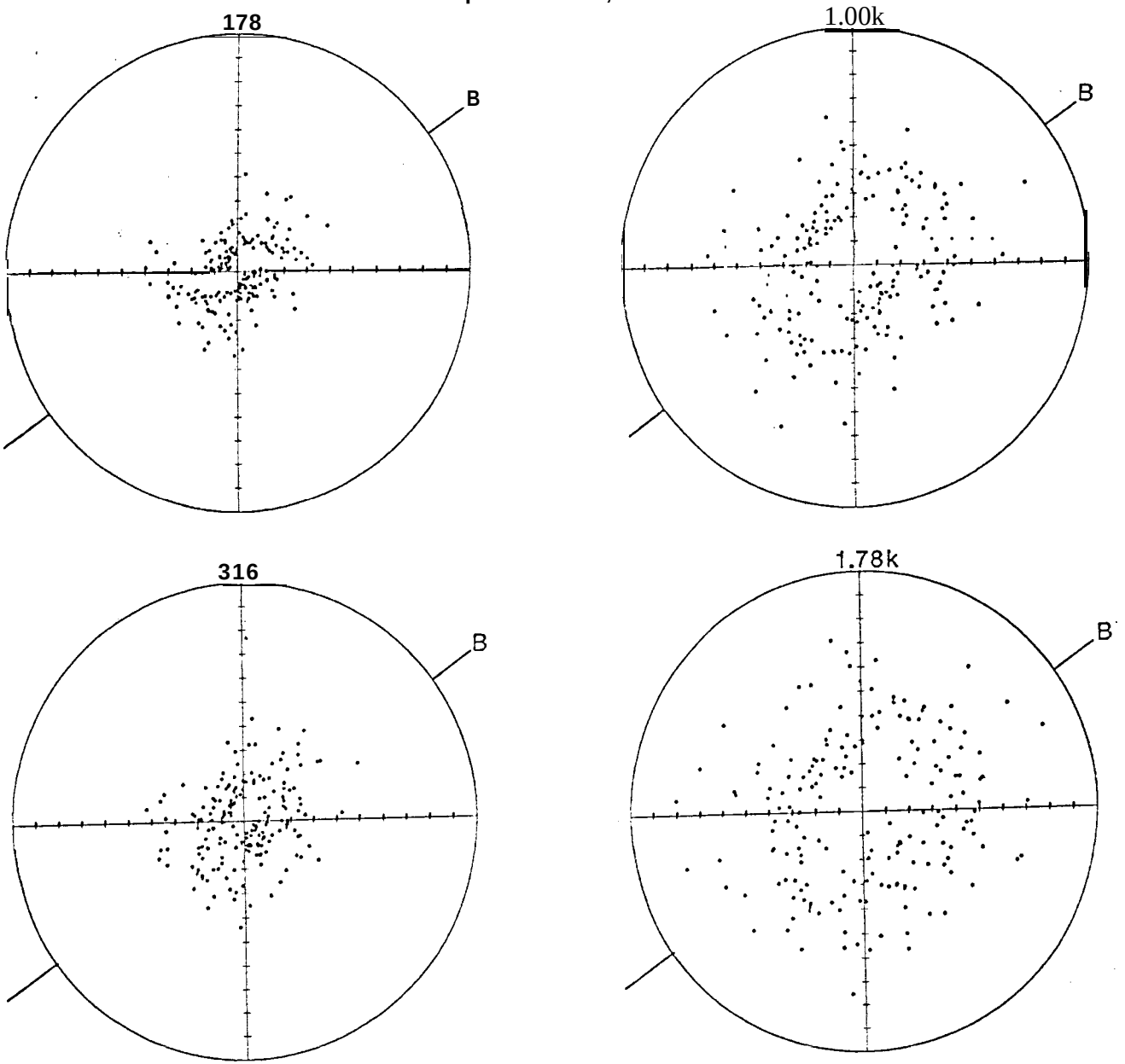

Fig 9a

ISEE-3 September 23, 1983 6:21:00

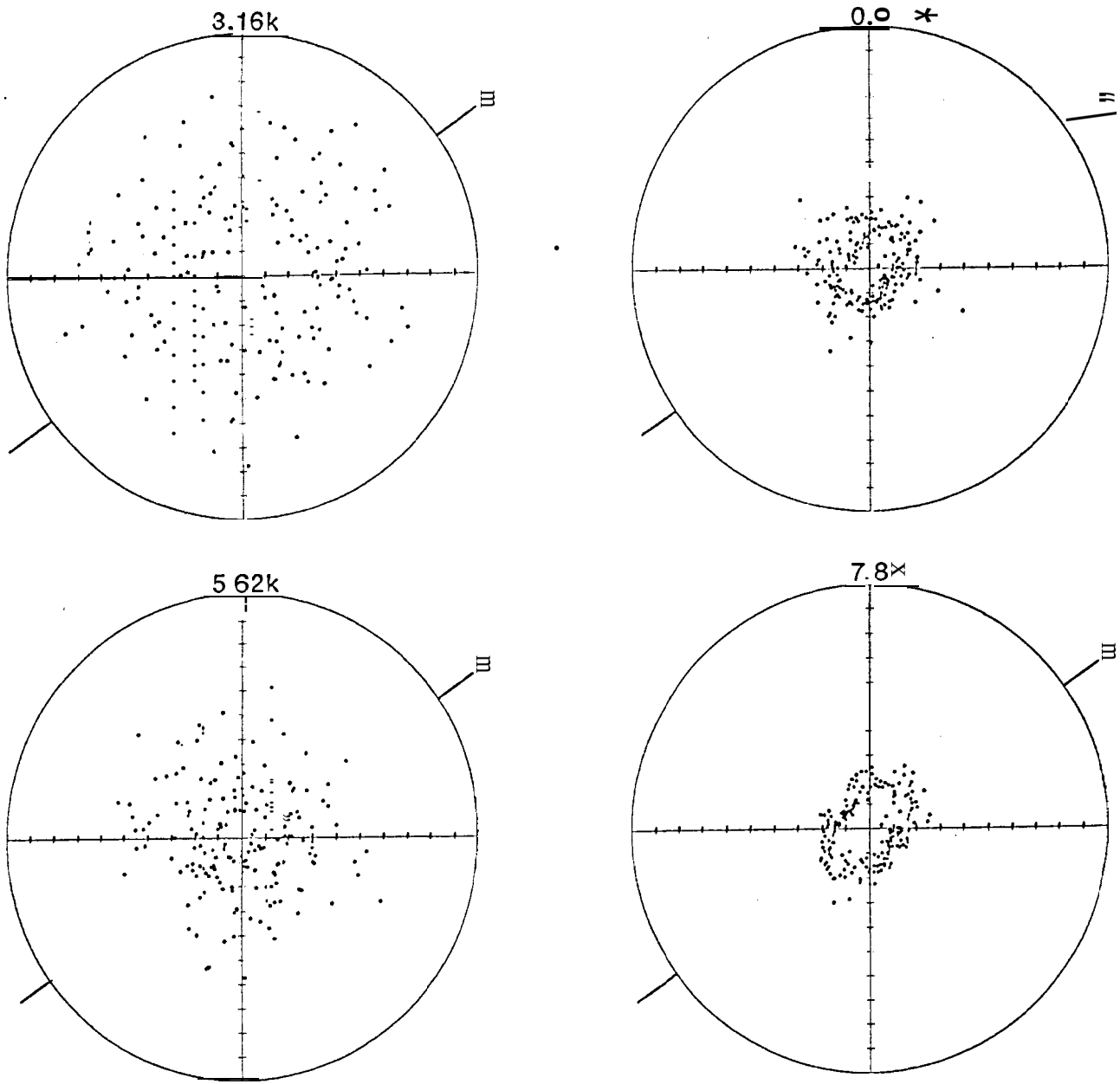

Fig. 9b

ISEE-3 September 22, 1983 17:03:30

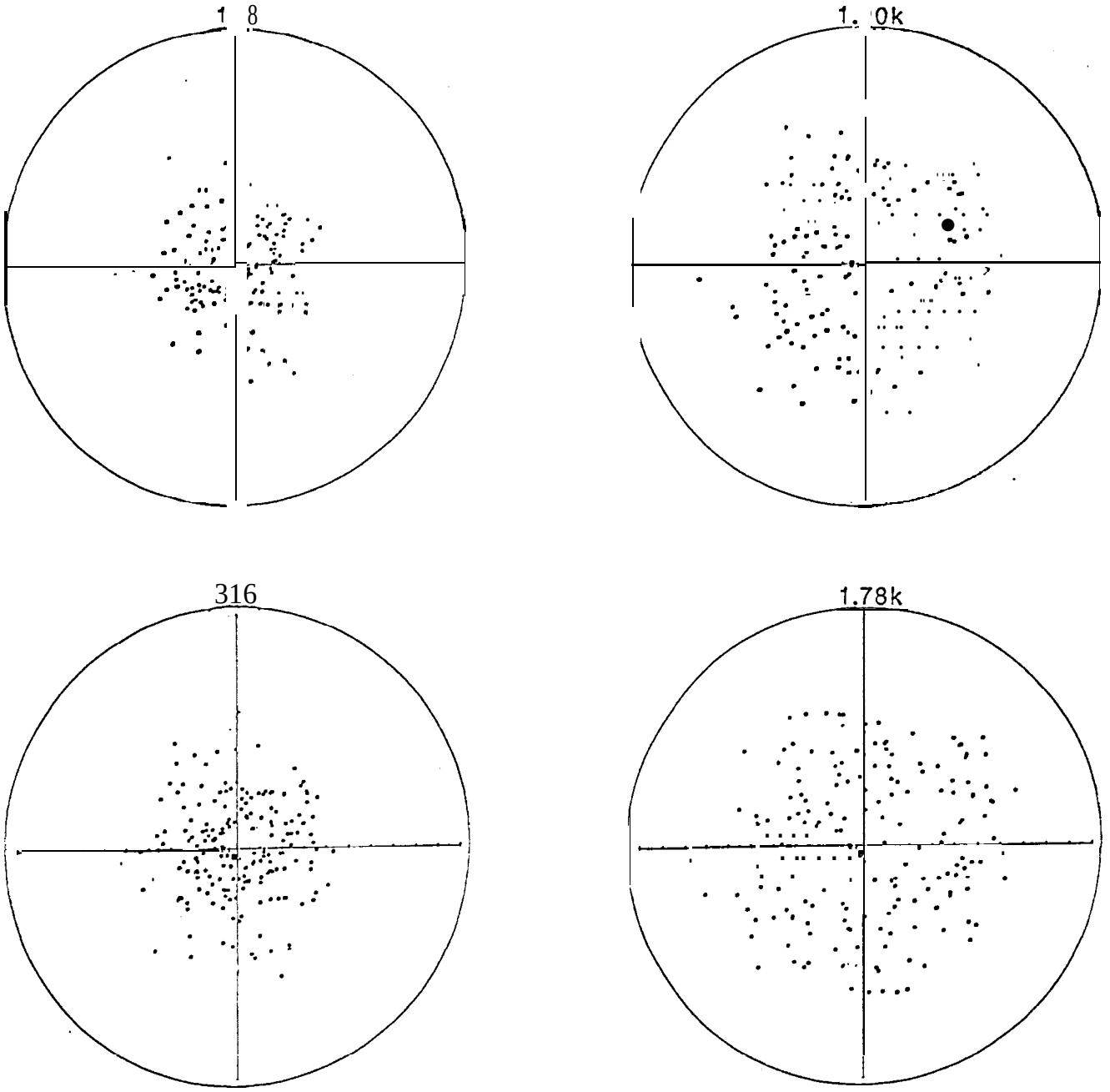

Fig. 10a

ISEE-3 September 22, 1983 17:03:30

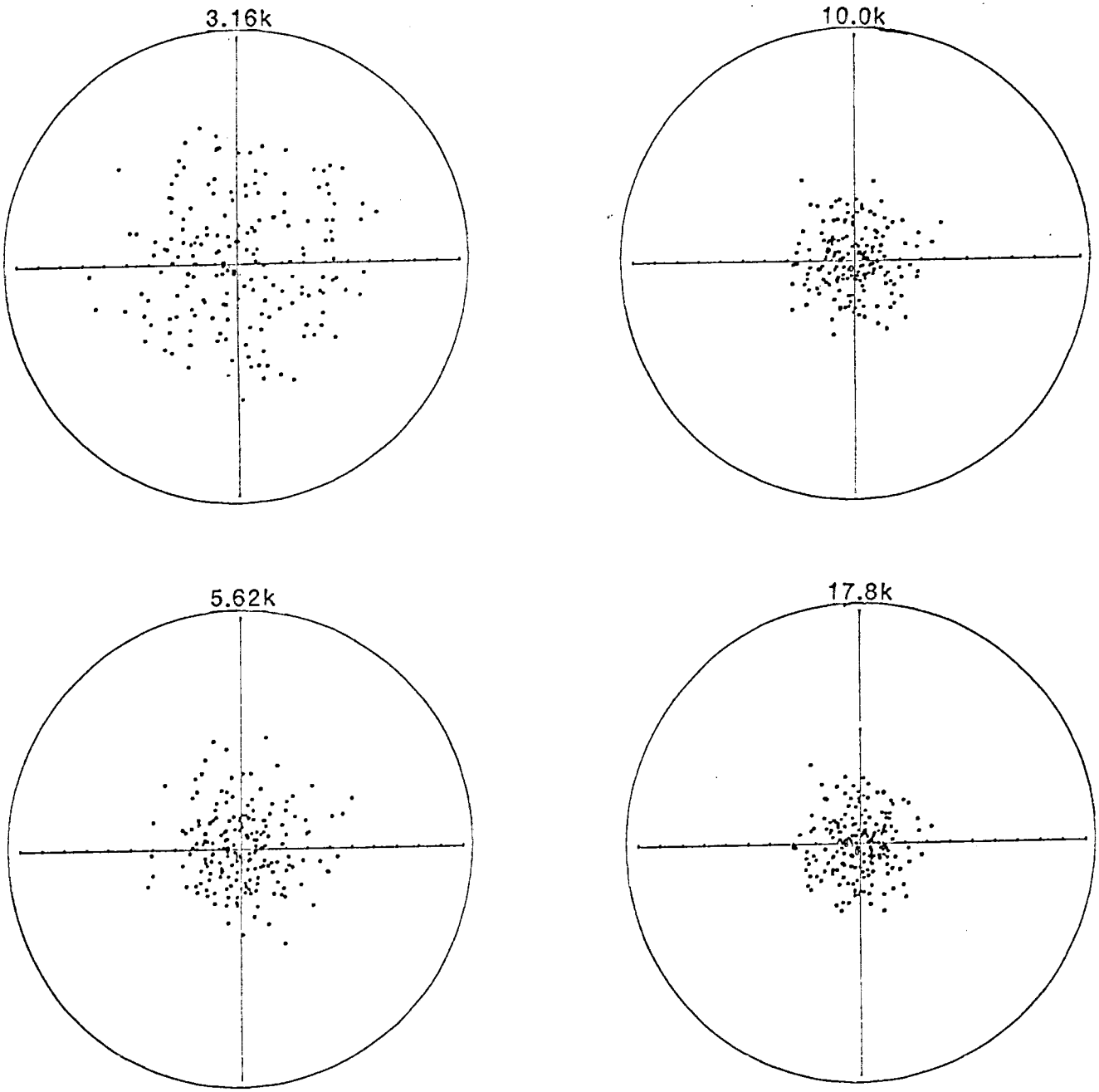

FIG. 10b

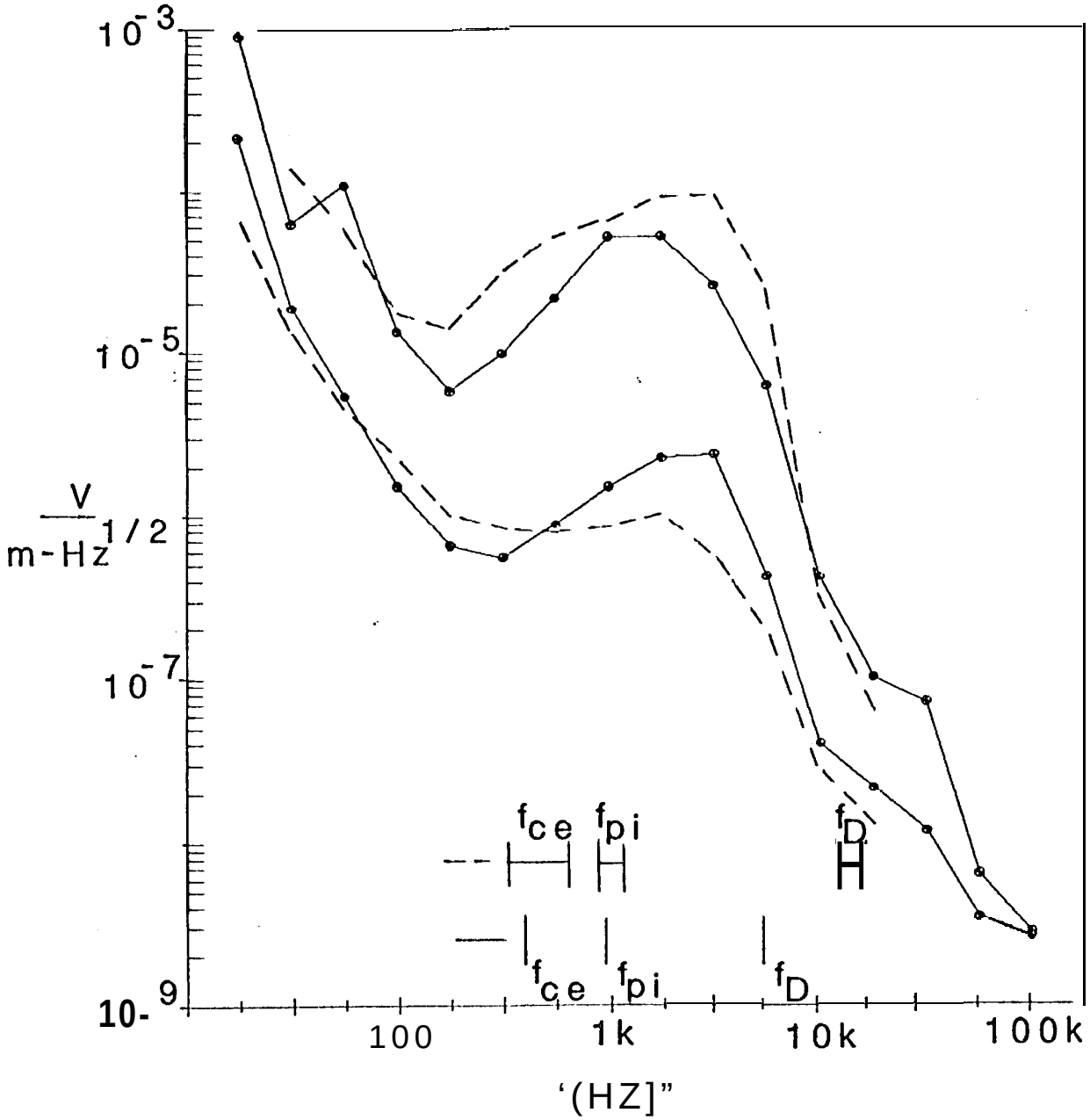

FIG. 11